



Designation: F2450 – 09

Standard Guide for Assessing Microstructure of Polymeric Scaffolds for Use in Tissue Engineered Medical Products¹

This standard is issued under the fixed designation F2450; the number immediately following the designation indicates the year of original adoption or, in the case of revision, the year of last revision. A number in parentheses indicates the year of last reapproval. A superscript epsilon (ϵ) indicates an editorial change since the last revision or reapproval.

1. Scope

1.1 This guide covers an overview of test methods that may be used to obtain information relating to the dimensions of pores, the pore size distribution, the degree of porosity, interconnectivity, and measures of permeability for porous materials used as polymeric scaffolds in the development and manufacture of tissue engineered medical products (TEMPs). This information is key to optimizing the structure for a particular application, developing robust manufacturing routes, and for providing reliable quality control data.

1.2 The values stated in SI units are to be regarded as standard. No other units of measurement are included in this standard.

1.3 *This guide does not purport to address all of the safety concerns, if any, associated with its use. It is the responsibility of the user of this standard to establish appropriate safety and health practices and to determine the applicability of regulatory limitations prior to use.*

2. Referenced Documents

2.1 ASTM Standards:²

D2873 Test Method for Interior Porosity of Poly(Vinyl Chloride) (PVC) Resins by Mercury Intrusion Porosimetry³

D4404 Test Method for Determination of Pore Volume and Pore Volume Distribution of Soil and Rock by Mercury Intrusion Porosimetry

E128 Test Method for Maximum Pore Diameter and Permeability of Rigid Porous Filters for Laboratory Use

E1294 Test Method for Pore Size Characteristics of Membrane Filters Using Automated Liquid Porosimeter³

F316 Test Methods for Pore Size Characteristics of Membrane Filters by Bubble Point and Mean Flow Pore Test

F2150 Guide for Characterization and Testing of Biomaterial Scaffolds Used in Tissue-Engineered Medical Products

3. Terminology

3.1 Definitions:

3.1.1 *bioactive agent, n*—any molecular component in, on, or within the interstices of a device that is intended to elicit a desired tissue or cell response.

3.1.1.1 *Discussion*—Growth factors and antibiotics are typical examples of bioactive agents. Device structural components or degradation byproducts that evoke limited localized bioactivity are not included.

3.1.2 *blind (end)-pore, n*—a pore that is in contact with an exposed internal or external surface through a single orifice smaller than the pore's depth.

3.1.3 *closed cell, n*—a void isolated within a solid, lacking any connectivity with an external surface. Synonym: *closed pore*

3.1.4 *hydrogel, n*—a water-based open network of polymer chains that are cross-linked either chemically or through crystalline junctions or by specific ionic interactions.

3.1.5 *macropore/macroporosity* (life sciences), *n*—a structure inclusive of void spaces sized to allow substantially unrestricted passage of chemicals, biomolecules, viruses, bacteria, and mammalian cells. In implants with interconnecting pores, provides dimensions that allow for ready tissue penetration and microvascularization after implantation. Includes materials that contain voids with potential to be observable to the naked eye ($>100\ \mu\text{m}$).

3.1.6 *micropore/microporosity* (life sciences), *n*—a structure inclusive of void spaces sized to allow substantially unrestricted passage of chemicals, biomolecules, and viruses while sized to control or moderate the passage of bacteria, mammalian cells, and/or tissue. Includes materials with typical pore sizes of greater than $0.1\ \mu\text{m}$ ($100\ \text{nm}$) and less than about $100\ \mu\text{m}$ ($100\ 000\ \text{nm}$), with a common microporous context encompassing the range of $20\ \mu\text{m}$ or less for the filtration of

¹ This guide is under the jurisdiction of ASTM Committee F04 on Medical and Surgical Materials and Devices and is the direct responsibility of Subcommittee F04.42 on Biomaterials and Biomolecules for TEMP.

Current edition approved June 1, 2009. Published July 2009. Originally approved in 2004. Last previous edition approved in 2004 as F2450–04. DOI: 10.1520/F2450-09.

² For referenced ASTM standards, visit the ASTM website, www.astm.org, or contact ASTM Customer Service at service@astm.org. For *Annual Book of ASTM Standards* volume information, refer to the standard's Document Summary page on the ASTM website.

³ Withdrawn. The last approved version of this historical standard is referenced on www.astm.org.

cells ranging from bacteria to common mammalian cells and above 30 micrometer for the ingrowth of tissue. Objects in this size range typically can be observed by conventional light microscopy.

3.1.7 *nanopore/nanoporosity* (life sciences), *n*—a structure inclusive of void spaces sized to control or moderate the passage of chemicals, biomolecules, and viruses while sized to substantially exclude most bacteria and all mammalian cells. Includes materials with typical pore sizes of less than 100 nm (0.1 μm), with common nanoporous context in the range of approximately 20 nm or less for the filtration of viruses.

3.1.8 *permeability*, *n*—a measure of fluid, particle, or gas flow through an open pore structure.

3.1.9 *polymer*, *n*—a long chain molecule composed of monomers including both natural and synthetic materials, for example, collagen, polycaprolactone.

3.1.10 *pore*, *n*—a fluid (liquid or gas) filled externally connecting channel, void, or open space within an otherwise solid or gelatinous material (for example, textile meshes composed of many or single fibers (textile based scaffolds), open cell foams, (hydrogels). Synonyms: *open-pore*, *through-pore*.

3.1.11 *porogen*, *n*—a material used to create pores within an inherently solid material.

3.1.11.1 *Discussion*—For example, a polymer dissolved in an organic solvent is poured over a water-soluble powder. After evaporation of the solvent, the porogen is leached out, usually by water, to leave a porous structure. The percentage of porogen needs to be high enough to ensure that all the pores are interconnected.

3.1.12 *porometry*, *n*—the determination of the distribution of open pore diameters relative to the direction of fluid flow by the displacement of a non-volatile wetting fluid as a function of pressure.

3.1.13 *porosimetry*, *n*—the determination of the pore volume and pore size distribution through the use of a non-wetting liquid (typically mercury) intrusion into a porous material as a function of pressure.

3.1.14 *porosity*, *n*—property of a solid which contains an inherent or induced network of channels and open spaces. Porosity can be determined by measuring the ratio of pore (void) volume to the apparent (total) volume of a porous material and is commonly expressed as a percentage.

3.1.15 *scaffold*, *n*—a support, delivery vehicle, or matrix for facilitating the migration, binding, or transport of cells or bioactive molecules used to replace, repair, or regenerate tissues.

3.1.16 *through-pores*, *n*—an inherent or induced network of voids or channels that permit flow of fluid (liquid or gas) from one side of the structure to the other.

3.1.17 *tortuosity*, *n*—a measure of the mean free path length of through-pores relative to the sample thickness. Alternative definition: The squared ratio of the mean free path to the minimum possible path length.

4. Summary of Guide

4.1 The microstructure, surface chemistry, and surface morphology of polymer-based tissue scaffolds plays a key role in encouraging cell adhesion, migration, growth, and proliferation. The intention of this guide is to provide a compendium of techniques for characterizing this microstructure. The breadth of the techniques described reflects the practical difficulties of quantifying pore sizes and pore size distributions over length scales ranging from nanometres to sub-millimetres and the porosity of materials that differ widely in terms of their mechanical properties.

4.2 These microstructural data when used in conjunction with other characterization methods, for example, chemical analysis of the polymer (to determine parameters such as the molecular weight and its distribution), will aid in the optimization of scaffolds for tissue engineered medical products (TEMPs). Adequate characterization is also critical to ensure the batch-to-batch consistency of scaffolds; either to assess base materials supplied by different suppliers or to develop robust manufacturing procedures for commercial production.

4.3 Application of the techniques described in this guide will not guarantee that the scaffold will perform the functions for which it is being developed but they may help to identify the reasons for success or failure.

4.4 This guide does not suggest that all listed tests be conducted. The choice of technique will depend on the information that is required and on the scaffold's physical properties; for example, mercury porosimetry will not yield meaningful data if used to characterize soft materials that deform during the test and cannot be used for highly hydrated scaffolds.

TABLE 1 A Guide to the Physical Characterization of Tissue Scaffolds

Generic Technique	Information Available	Section
Microscopy	Pore shape, size and size distribution, porosity.	6.1 (Electron microscopy) 6.2 (Optical microscopy) 6.2.2 (Confocal microscopy) 6.2.3 (Optical coherence tomography) 6.2.4 (Optical coherence microscopy)
X-Ray Micro-computed Tomography (MicroCT)	Pore shape, size and size distribution, porosity.	6.3
Magnetic Resonance Imaging	Pore shape, size and size distribution, porosity.	6.4
Measurement of density	Porosity, pore volume	7.2
Porosimetry	Porosity, total pore surface area, pore diameter, pore size distribution	7.3
Porometry	Median pore diameter (assuming cylindrical geometry), through-pore size distribution	7.4
Diffusion of markers	Permeability	8.2
NMR	Pore size and distribution	8.3

4.5 **Table 1** provides guidance for users of this guide by providing a brief overview of the applicability of a range of different measurement techniques that can be used to physically characterize tissue scaffolds. This list of techniques is not definitive.

5. Significance and Use

5.1 The ability to culture functional tissue to repair damaged or diseased tissues within the body offers a viable alternative to xenografts or heterografts. Using the patient’s own cells to produce the new tissue offers significant benefits by limiting rejection by the immune system. Typically, cells harvested from the intended recipient are cultured *in vitro* using a temporary housing or scaffold. The microstructure of the scaffold, that is, its porosity, the mean size, and size distribution of pores and their interconnectivity is critical for cell migration, growth and proliferation (**Appendix X1**). Optimizing the design of tissue scaffolds is a complex task, given the range of available materials, different manufacturing routes, and processing conditions. All of these factors can, and will, affect the surface roughness, surface chemistry, and microstructure of the resultant scaffolds. Factors that may or may not be significant variables depend on the characteristics of a given cell type at any given time (that is, changes in cell behavior due to the number of passages, mechanical stimulation, and culture conditions).

5.2 Tissue scaffolds are typically assessed using an overall value for scaffold porosity and a range of pore sizes, though the distribution of sizes is rarely quantified. Published mean pore sizes and distributions are usually obtained from electron microscopy images and quoted in the micrometer range. Tissue scaffolds are generally complex structures that are not easily interpreted in terms of pore shape and size, especially in three-dimensions. Therefore, it is difficult to quantifiably assess the batch-to-batch variance in microstructure or to enable a systematic investigation to be made of the role that the mean pore size and pore size distribution has on influencing cell behavior based solely on electron micrographs (Tomlins et al, **(1)**).⁴

5.2.1 **Fig. 1** gives an indication of potential techniques that can be used to characterize the structure of porous tissue scaffolds and the length scale that they can measure. Clearly a range of techniques must be utilized if the scaffold is to be characterized in detail.

5.2.2 The classification and terminology of pore sizes, such as those given in **Table 2**, has yet to be standardized, with definitions of terms varying widely (as much as three orders of magnitude) between differing applications and industries. Both

⁴ The boldface numbers in parentheses refer to the list of references at the end of this standard.

Pore Size Characterization Techniques

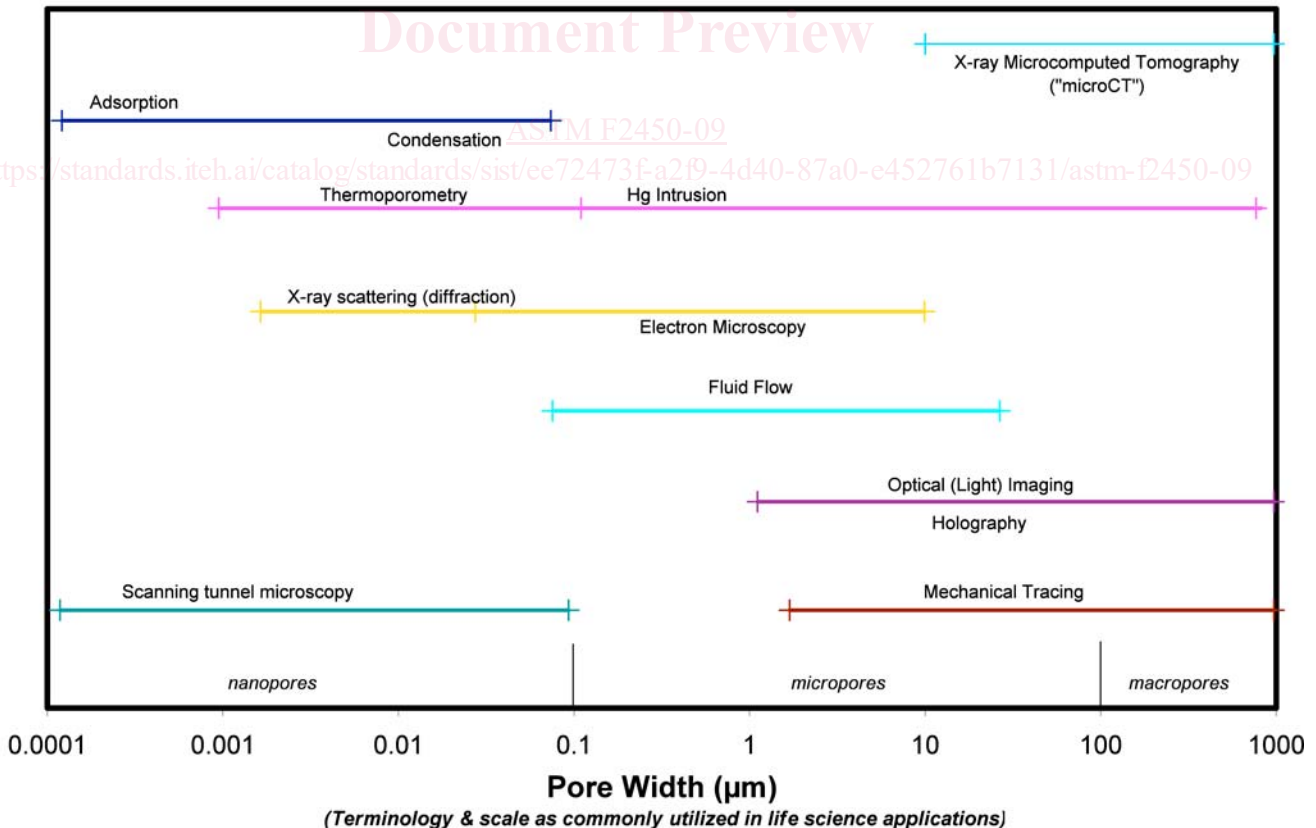


FIG. 1 A Range of Techniques is Required to Fully Characterize Porous Materials
(Note—Figure redrawn from Meyer (2).)

TABLE 2 Comparison of Pore Size Nomenclature

Descriptor	IUPAC Definitions	Definitions for Life Science Applications
	<i>For: chemical (for example, solid catalysts); metallurgy; geology (for example, zeolites) applications</i>	<i>For: tissue engineering; medical implants; diagnostic or biological filtration applications</i>
Nanopore/nanoporosity	Not utilized	0.002 to 0.1 μm (2 to 100 nm)
Micropore/microporosity	<2 nm (<20 \AA)	0.1 to 100 μm (typically defined 0.1 to 20 μm)
Mesopore	2 to 50 nm (20 to 500 \AA)	Not utilized
Macropore/macroporosity	>50 nm (>500 \AA)	>100 μm
Capillaries	Meyer, et al. (2)	Not utilized
Macrocapillaries	Meyer, et al. (2)	Not utilized

Table 2 and the supporting detailed discussion included within **Appendix X2** describe differences that exist between IUPAC (International Union of Pure and Applied Chemistry) definitions and the common terminology currently utilized within most life science applications, which include both implant and tissue engineering applications..

5.2.2.1 Since the literature contains many other terms for defining pores (Perret et al (3)), it is recommended that the terms used by authors to describe pores are defined in order to avoid potential confusion. Additionally, since any of the definitions described within **Table 2** can shift dependent on the pore size determination method (see **Table 1** and **Fig. 1**), an accompanying statement describing the utilized assessment technique is essential.

5.2.3 All the techniques listed in **Table 1** have their limitations for assessing complex porous structures. **Fig. 2a** and **Fig. 2b** show a through- and a blind-end pore respectively. Porometry measurements (see 7.4) are only sensitive to the narrowest point along a variable diameter through-pore and therefore can give a lower measure of the pore diameter than other investigative techniques, such as SEM, which may sample at a different point along the pore. The physical basis of porometry depends on the passage of gas through the material. Therefore, the technique is not sensitive to blind-end or enclosed pores. Therefore, estimates of porosity based on porometry data will be different to those obtained from, for example, porosimetry (see 7.3), which is sensitive to both through- and blind-pores or density determinations that can also account for through-, blind-end, and enclosed pores. The significance of these differences will depend on factors such as the percentage of the

different pore types and on their dimensions. Further research will enable improved guidance to be developed.

5.2.4 Polymer scaffolds range from being mechanically rigid to those that are soft hydrogels. The methods currently used to manufacture these structures include, but are not limited to:

5.2.4.1 Casting a polymer, dissolved in an organic solvent, over a water-soluble particulate porogen, followed by leaching.

5.2.4.2 Melt mixing of immiscible polymers followed by leaching of the water-soluble component.

5.2.4.3 Dissolution of supercritical carbon dioxide under pressure into an effectively molten polymer, a phenomenon attributed to the dramatic reduction in the glass transition temperature which occurs, followed by a reduction in pressure that leads to the formation of gas bubbles and solidification.

5.2.4.4 Controlled deposition of molten polymer to produce a well-defined three-dimensional lattice.

5.2.4.5 The manufacture of three-dimensional fibrous weaves, knits, or non-woven structures.

5.2.4.6 Chemical or ionic cross-linking of a polymeric matrix.

5.2.5 Considerations have been given to the limitations of these methods in **Appendix X1**.

5.2.6 This guide focuses on the specific area of characterization of polymer-based porous scaffolds and is an extension of an earlier ASTM guide, Guide **F2150**.

6. Imaging

6.1 *Electron Microscopy*—Both transmission and scanning electron microscopy can be used to image intact or fractured

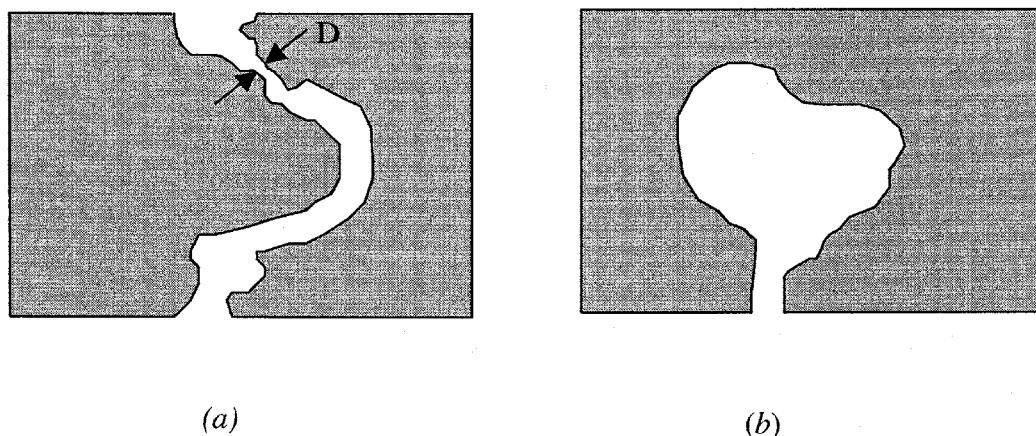


FIG. 2 A through-pore showing a variation of pore diameter, D (a); and an example of a blind-pore (b).

surfaces or sections cut from tissue scaffolds. The resultant images can be interpreted using image analysis software packages to generate data concerning the shape of pores within the scaffold, their mean size, and distribution. Estimates of both permeability and tortuosity can be made from three-dimensional virtual images generated from transmission electron microscopic images of serially sectioned samples.

6.1.1 There is likely to be a high degree of uncertainty in the reliability of quantitative data derived from electron microscopic examination of soft or especially highly hydrated soft polymer-based scaffolds due to the presence of artifacts created during sample preparation. These problems may be overcome by using environmental scanning electron microscopy. Highly hydrated scaffolds need to be freeze-dried before examination under vacuum in a conventional scanning electron microscope. This process, if carried out in liquid nitrogen, usually results in a significant amount of ice damage due to the relatively slow cooling rates that are encountered due to the thin layer of insulating nitrogen gas that forms around the sample as it is frozen. Freezing samples in slush nitrogen can reduce ice damage by enabling faster cooling rates by apparently reducing the thickness of the insulating gas layer.

6.1.2 Polymer-based scaffolds often lack sufficient electron density to provide suitable levels of contrast; this can be overcome by staining using a high electron density material such as osmium tetroxide that has a high affinity for carbon-carbon double bonds.

6.1.3 Most polymer-based scaffolds can be mounted in epoxy resin using standard procedures and subsequently sectioned for serial examination in the transmission electron microscope. This method is less appropriate for investigating hydrogels that can be gradually dehydrated using a series of alcohol solutions, following standardized procedures, before embedding. However, this procedure tends to reduce the size of the water-filled pores within the sample. The quantifiable pore size data subsequently obtained are of value if microstructural comparisons between different samples are required. Consequently, these data are likely to be inappropriate for characterizing the microstructure of samples per se due to the artifacts.

6.2 *Optical Microscopy-Based Methods:*

6.2.1 *Optical (Light) Microscopy*—Images of the surfaces of tissue scaffolds can be obtained using an optical microscope. This technique enables surface features to be studied with minimal preparation in a ‘natural’ state (that is, the specimen does not need to be stained or sectioned). This examination is simplified if the specimen is illuminated from above. For thin specimens or materials lacking in opacity, the resultant images may be difficult to interpret due to lack of clarity that is attributable to the underlying structure. In some cases, differential focus can be used to collect images at different depths within semi-transparent specimens, providing that there is sufficient contrast and detail in the images. These deep view images can be used to track the path of interconnected pores within the sample.

6.2.2 *Confocal Microscopy*—Substantial improvements in the quality of ‘optically’ sectioned samples can be made by either exploiting the fluorescent properties that the scaffold may have or by introducing a fluorophore into it. Confocal

microscopy can capture well-resolved images at different depths because of its shallow depth of field and elimination of out-of-focus glare. A laser is usually used as a point light source in preference to a conventional lamp. Laser scanning confocal microscopy (LSCM) is used extensively in the biomedical arena. LSCM utilizes a variable sized pinhole to reject the image out-of-plane scatter (that is, glare) and can be utilized in reflection or transmission modes. The size of the pinhole and the numerical aperture of the objective primarily determine the resolution in the thickness or axial direction. Generally, smaller holes give better resolution but at the expense of reduced intensity.

6.2.2.1 Some work has been reported on scaffold characterization using laser scanning confocal microscopy (LSCM) (Tjia and Moghe, (4), Birla and Matthew (5)). Using LSCM, the image depth is limited to a couple of layers of pores because of the relatively ineffective way LSCM rejects stray (background) light.

6.2.3 *Optical Coherence Tomography*—Optical Coherence Tomography (OCT) is a reflectance optical imaging technique that uses interferometric rejection of out-of-plane scattering of photons rather than a pinhole as in LSCM to determine axial resolution. Briefly, OCT uses a low coherence source with a bandwidth of anywhere from 30 to 200 nm and an interferometer, usually of Michelson type, that generates profiles of back-reflected light for any one transverse position. For a complete description of OCT and its applications, see Ref (21). An analogous technique is ultrasound A-scanning. In the Michelson configuration, the material is the fixed arm of the interferometer rather than a mirror. A low numerical aperture lens is used to achieve a large axial sampling volume and reflections from heterogeneities within the sample are mapped as a function of thickness for any one position. Like LSCM, transverse resolution is determined by geometric optics. Unlike LSCM, axial resolution is inversely proportional to the bandwidth of the source, and a typical value for axial resolution is 10 μm . Volume information is generated by translating the sample on a motorized stage.

6.2.3.1 The advantage of OCT is that it is highly sensitive, typically 90 dB. OCT has been extensively used to image the human retina (Hee et al (6)), skin and blood vessels (Barton et al (7)), and the operating circulatory system of small live animals (Boppart et al (8)) with excellent clarity. In the late 1990s, the potential for OCT was seen in the area of materials science. The first published OCT images of a tissue-engineering scaffold are of a hydrogel and demonstrate the depth to which images can be obtained (McDonough et al (9)). The depth of field of the image is limited by scattering from the pores and any crystallites that are present. It can vary from approximately 100 μm to several millimetres depending on the difference in refractive index between the material and its surroundings, the level of porosity, and the pore size distribution. The penetration depth can be improved by filling the pores with a fluid of similar refractive index to the scaffold material. In practice, this is usually a substitution of water for air or oil for water. This procedure can result in additional problems due to poor wetting and trapped air. OCT images of porous materials tend to be noisy due to multiply scattered

photons that contribute to the signal. A related technique, optical coherence microscopy, overcomes the issues related to the fidelity of imaging tissue-engineering scaffolds.

6.2.4 Optical Coherence Microscopy—Optical coherence microscopy (OCM) is a combination of OCT and confocal microscopy. OCM is highly suited for imaging of optically opaque materials such as tissue engineering scaffolds because it can attain axial and transverse resolution on the order of a micrometer and still maintain high background rejection. The confocal enhancement is done in the usual manner by the addition of a high numerical aperture objective and a pinhole, which is usually the open aperture of the sample arm fiber. For more information on OCM, see Ref (21). The key to the technique is the axial point spread functions (PSF) of the confocal and coherence techniques. For the confocal component, the Lorentzian axial PSF results in a finite collection efficiency even far out of the focus plane, and this limits its use in highly scattering media such as TEMPs. For the coherence component, the Gaussian PSF drops off far from the focal plane much more rapidly than that of confocal microscopy. Hence, the confocal component contributes to the high resolution near the focus and the coherence component contributes to the high background rejection, two qualities needed for effective imaging of TEMPs (Dunkers et al (10)). With confocal enhancement, the typical axial resolution of OCT of approximately 10 to 20 μm can be increased approximately 10 fold to 1.5 to 2 μm with no loss of the depth of field.

6.3 X-Ray Micro-computed Tomography (MicroCT)—X-rays can be used to generate three-dimensional images of tissue scaffolds from which information on pore size and shape, porosity, and interconnectivity can be obtained. The principle of the method is to position the scaffold between an x-ray source and a detector. The x-ray beam is typically around 5 μm in diameter. The sample is rotated and the x-ray attenuation is recorded at a number of different angles. These data can then be analyzed using reconstruction algorithms to produce an image of a two-dimensional slice through the scaffold. A full three-dimensional image can be generated from a series of two-dimensional slices obtained at different heights within the sample. Typical resolution of such an image is around 10 μm , but this value is continually being improved. The success of the technique relies on there being sufficient contrast, that is, differences in electron density between the solid material and a fluid (typically air or water) within the pores.

6.3.1 The technique does not suffer from the same penetration depth limitations that optical tomographic methods suffer from, providing a more complete picture of the scaffold structure. The non-destructive approach has been used to investigate the structure of bone and other materials (Muller et al, (11), Muller et al, (12)) to validate the design of bone scaffolds (Van Oosterwijck et al, (13)) and investigate polymeric scaffolds (Maspero et al (14), Lin et al (15)).

6.4 Magnetic Resonance Imaging—Many polymers contain MR active nuclei (for example, ^1H , ^{13}C), but the relaxation times of nuclei on the polymer backbone are too short for routine imaging applications. Thus, to study the three-dimensional morphology of polymeric scaffolds, the pore space must be filled with a fluid, which is visible in the

magnetic resonance imaging (MRI) experiment. The ideal fluid must contain MR active nuclei, which are naturally abundant, have a high receptivity, and have a well-resolved NMR spectrum of narrow lines. Moreover, it needs to have a low viscosity to infiltrate the pore space and must have appropriate relaxation properties to provide a large signal, after the application of the imaging gradients. Fortunately, immersion in water will suffice for most polymeric scaffolds.

6.4.1 The theoretical limit in spatial resolution for MRI experiments is typically the distance a water molecule diffuses during the time it takes to acquire the MRI signal, $\sim 10 \mu\text{m}$. Thus, polymeric scaffolds with large pores (50 to 100 μm) can be spatially resolved with this technique. In MR images, the water-filled pores appear bright and the polymer mesh dark. High contrast images of the polymer mesh, after suitable image analysis, can be used to generate estimates of pore sizes and pore size distribution.

6.4.2 The porosity of scaffolds that have pores that are smaller than the resolution limit of the MRI technique can be estimated from the signal intensity of a water-saturated scaffold normalized to that of pure water. The normalized signal intensity reflects the volume fraction of water present within the polymer scaffold, if the polymer does not contribute to measured signal. For hydrogels, a better estimate of the polymeric volume fraction can be derived from quantitative transverse relaxation maps. This approach is used to analyze the density of cross-links in hydrogels used as radiation dosimetry phantoms. For polymeric scaffolds with pore sizes comparable to the diameter of a cell (10 to 20 μm), MR images of the diffusion behaviour of the pore fluid can yield estimates of the pore size and size distribution. A limitation of this approach is the need to assume a geometric model to obtain structural information.

6.4.3 Other limitations of the MRI technique include its low spatial resolution and the necessity of a pore fluid to study the structure of the scaffold, which limits the technique to detecting only those pores that are fluid filled. In practice, MRI will be unable to detect enclosed pores or those which either trap air—blind-end pores—or are difficult to wet out due to surface tension. The distribution of the pore fluid within the scaffold is a potential measure of pore volume accessible to cells although lack of signal in certain regions can be attributed to trapped air, solid polymer, or the presence of small diameter dry pores.

6.4.4 The advantage of the MRI technique is that polymeric scaffolds can be non-destructively investigated in three-dimensions, without the need for using stains or dyes. The scaffold does not need to be optically transparent and preparative techniques, which can alter the morphology of the polymeric scaffold, are not required. Additionally, this imaging modality can be used to monitor the distribution of cells and extracellular matrix proteins within the scaffold, both spatially and temporally. Furthermore, MRI can monitor the performance of a tissue scaffold *in vivo* as well as the biological response of the body to the scaffold material.

6.5 Image Analysis—Irrespective of which technique is used to image tissue scaffolds, it is imperative that due consideration is given to the quantitative determination of key structural parameters. Typically the porous regions within a